VIRTUAL INSTRUMENTS FOR DETECTING ROTOR FAULTS IN INDUCTION MOTORS

L. Szabó, J. B. Dobai, K. Á. Biró
Technical University of Cluj
400750 Cluj, P.O. Box 358, Romania
e-mail: Lorand.Szabo@mae.utcluj.ro

Summary Rotating electrical machines play an important role in the world's industrial life. Hence there is a strong demand on their reliable and safe operation. Their faults and failures can lead to excessive downtimes and generate enormous costs in reduced output, emergency maintenance and lost revenues. Therefore the fault detection methods of electrical machines are of real interest. For the rotor faults diagnosis of induction machines one of the most widely used methods is the so-called motor current signature analysis (MCSA). This method can be applied both to the squirrel-cage and to the wound rotor induction motors. For current measurements and data processing virtual instruments are proposed. In this paper some results obtained in the case of the wound rotor induction machine will be presented.

1. INTRODUCTION

The most commonly used motor in industrial applications is the three-phase induction motor due to its several advantages as simple design, rugged construction, reliable operation, low initial cost, easy operation and maintenance, relatively high efficiency, etc. Most of the utilised induction motors are of squirrel-cage rotor, but also numerous wound rotor induction motors are used.

The wound rotor (also called the slip-ring motor) has nearly the same stator construction and winding arrangement as the squirrel-cage induction motor: a three-phase winding placed in the slots of a laminated steel core.

The cylindrical core of its rotor is made up of steel laminations, slotted to hold the formed coils of the three star connected single-phase windings. The coils of the rotor winding are grouped to form the same number of poles as in the stator windings. The three leads from these windings terminate at three slip rings mounted on the rotor shaft. Carbon brushes press against these slip rings and are held securely by adjustable springs mounted in the brush holders. The brush holders are fixed rigidly. Leads from the carbon brushes are usually connected to an external speed controller.

Also this type of electrical machine has some advantages. Because of they high starting torque (of 200÷250% of the full load torque) and relatively low starting current (250÷350% of the full load current) the wound rotor induction machines are often used in those constant speed drives where great starting torque is required. Its speed can be controlled simply (but with low efficiency) by regulating rotor resistance.

In these applications the failures of the wound rotor induction motors can shut down an entire industrial process. Such unplanned machine shut downs cost both time and money that could be avoided if an early warning system should be available against impending failures [1].

Hence precise fault diagnosis methods applied to this class of electrical machines could improve process safety, a key factor in many industrial environments.

One of the most frequently used fault detection methods is the motor current signature analysis (MCSA). This technique depends upon locating by spectrum analysis specific harmonic components in the line current produced of unique rotating flux components caused by faults such as broken rotor bars, air-gap eccentricity and shorted turns in stator windings, etc. Note that only one current transducer is required for this method, and it can be in any one of the three phases. The motor current signature analysis method can detect these problems at an early stage and thus avoid secondary damage and complete failure of the motor. Another advantage of this method is that it can be also used online [2, 3].

The motor current signature analysis method can be applied both for the squirrel-cage and for the wound rotor induction motors. Several papers were presented in the field of applying the current signature method for squirrel-cage induction machines. Nevertheless there were not found any reports on applying this method for wounded rotor induction machines. Therefore the results presented in this paper may be of real interest for all the specialists involved in this field of electrical engineering.

2. THE LABORATORY SETUP

In order to perform the required measurements a test bench was set up in the laboratory of our Department (see Fig. 1.).

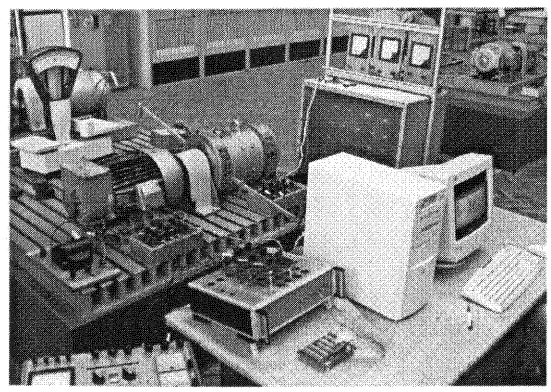

Fig. 1. The laboratory setup.

The test bench consists of two mechanically coupled electric motors, a dc motor for breaking and loading purposes and the induction motor to be tested. Voltage and current sensors give signals to the data acquisition board.

The measurement part of the bench consists of a usual Pentium processor based PC having a National Instruments AT-MIO-16XE-10 type acquisition board. This delivers high performance and reliable data acquisition capabilities, having 1.25 MS/s sampling rate, 16 single-ended analogue inputs. It features both analogue and digital triggering capability, as well as two 12-bit analogue outputs, two 24-bit, 20 MHz counter/timers and eight digital I/O lines. The electrical signals generated by the transducers are optimised for the input range of the DAQ board. The SCXI 1140 type signal conditioning accessory amplifies the low-level signals, and then isolates and filters them for more accurate measurements [4].

LabVIEW 6i programs (virtual instruments) co-ordinate all the data acquisition and the testing processes.

The tested wound rotor induction motor (shown in Fig. 2.) is of M2-3/6 type and has the following main data:

- Rated power: 3 kW
- Rated voltage: 220/380 V (Δ/Y)
- Rated current: 13,9/8 A (Δ/Y)
- Rated speed: 920 r/min.

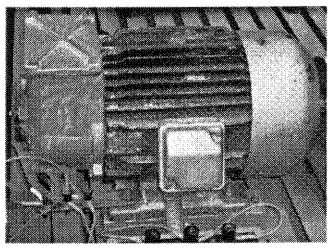

Fig. 2. The tested motor.

The presented test bench can be used also for testing other types of electrical machines.

3. THE VIRTUAL INSTRUMENTS

In modern laboratories the analogue and digital instruments can be replaced with custom-written virtual instruments (VI), which can be delivered by computers. This way the users can benefit of the high-performance computation and display capabilities of the modern computers [5].

Virtual instruments feature great flexibility, leaving instrument definition in the hands of the user, who can easily combine a number of general-purpose hardware instruments with the processing capabilities of a computer and/or DSP hardware to create specialised instruments. These virtual instruments can be easily reconfigured for other applications.

LabVIEW is a powerful graphical programming development for data acquisition and control, data analysis and data presentation. It is ideal for creating virtual instruments. LabVIEW features a well-defined strategy for constructing both hardware and software modules that are easy to understand and maintain. The virtual instruments can be rapidly combined, interchanged, and shared to build custom applications. Different hardware acquisition options can feature drop-in replacement virtual instruments for truly modular application development.

Several special virtual instruments were built up in LabVIEW 6i graphic programming environment. All of them were simply made by assembling using drag-and-drop methods software objects from the various libraries of the program.

From the numerous virtual instruments created here only a single one will be presented in Fig. 3.

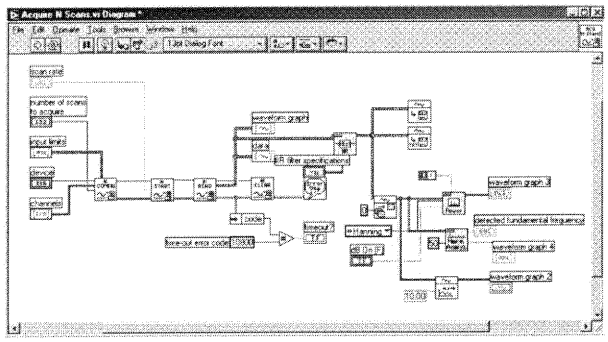

Fig. 3. The diagnosing virtual instrument's block diagram.

This program (a virtual instrument) acquires the three phases of the induction motor's stator current. The measured current of a single phase is processed. By means of Fast Fourier Transform (FFT) the time domain data is transformed into frequency domain. In the power spectrum of the measured line current its harmonic content can be studied.

The acquired data also can be stored in simple ASCII-type text files in order to be easy imported in any other programming environment.

4. RESULTS

Several measurements were performed using the above described test bench and the computer programs.

The wound rotor motor was tested when it was considered healthy and with a provoked rotor fault. The rotor fault was simulated by interrupting a rotor phase. In both cases the induction motor was tested at no-load condition and at three different loads.

The sample frequency for the data acquisition was set to a high value (2^{16}=65.536 samples/seconds), in order to make possible the observation also of the higher frequency harmonics. One second long measurement was performed, which means that on each channel 65.536 values were saved.

As it was observed, at no-load the effects of the fault couldn't be clearly observed, since the currents in the rotor windings are small. The most eloquent results were obtained at great loads, especially near the rated load.

The measured line currents for the healthy and faulty wound rotor induction machine at three loads are given in Fig. 4.

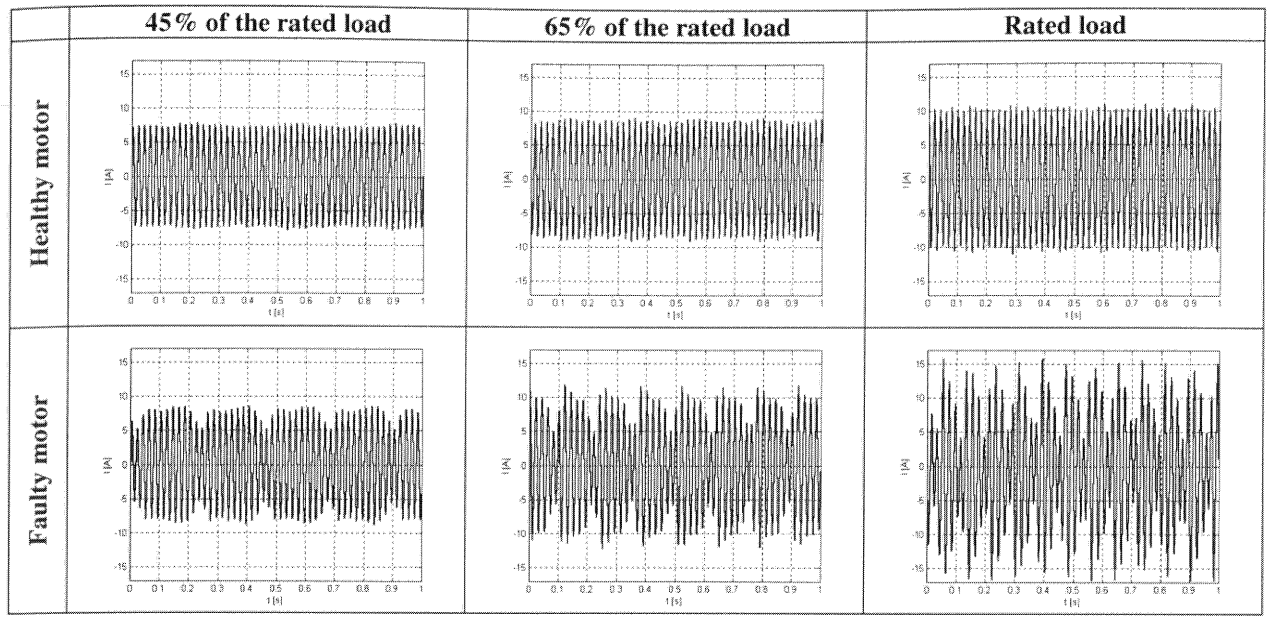

Fig. 4. The measured line currents of the tested wound rotor induction motor.

As it can be clearly seen in the figure the magnitude of the currents is intensifying with the increase of the load.

Beside this inherent effect a pronounced fluctuation of the line currents can be also observed in the case of the induction motor having a rotor fault.

This phenomena easily can be explained: in the three-phase induction motor under perfectly balanced conditions (healthy motor) only a forward rotating magnetic field is produced, which rotates at synchronous speed, $n_1 = f_1/p$, where f_1 is the supply frequency and p the pole-pairs of the stator windings.

When a rotor fault appears the three-phase system becomes unbalanced and an additional, a backward rotating magnetic field is produced, which is rotating at the slip speed, $n_2 = n_1(2s-1)$, with respect to the stator.

The pulsation's speed of the resulting magnetic flux and also of the line currents is given by the sum of the above mentioned two speeds: $n_p = n_1 + n_2 = 2n_1 s$.

As it was stated out previously the basis of the current signature analysis is the detection of those (so-called sideband) harmonic components of the measured line current which are significantly increased when a fault appears in the motor.

Upon the theoretical expectations in the case of the wound rotor induction motor having rotor faults the significant sideband frequencies are given by:

$$f = f_1(\nu + 2ks), \quad \nu = 1, 3, 5\ldots, \quad k = \pm 1, 2, 3\ldots \qquad (1)$$

where ν is the harmonics order and k an integer number.

The expected increased sideband frequencies computed upon (1) are given in Table 1.

Tab. 1. The analytically computed frequencies of the sideband harmonics.

	The frequencies of the significant sideband harmonics [Hz]		
	45% of the rated load	**65% of the rated load**	**Rated load**
Speed [r/min]	955	925	880
Slip [–]	0.045	0.075	0.120
ν=1, k=1 and k=-1	54.50, 45.50	57.50, 42.50	62.00, 38.00
ν=1, k=2 and k=-2	59.00, 41.00	65.00, 35.00	74.00, 26.00
ν=1, k=3 and k=-3	63.50, 36.50	72.50, 27.50	86.00, 14.00
ν=3, k=1 and k=-1	154.50, 145.50	157.50, 142.50	162.00, 138.00
ν=3, k=2 and k=-2	159.00, 141.00	165.00, 135.00	174.00, 126.00
ν=3, k=3 and k=-3	163.50, 136.50	172.50, 127.50	186.00, 114.00
ν=5, k=1 and k=-1	254.50, 245.50	257.50, 242.50	262.00, 238.00
ν=5, k=2 and k=-2	259.00, 241.00	265.00, 235.00	274.00, 226.00
ν=5, k=3 and k=-3	263.50, 236.50	272.50, 227.50	286.00, 214.00

After the Fourier transform (FFT) applied the power spectrum of the measured line currents were obtained. For a better view and for a correct comparison to make the ratio in decibels of the measured current and of the rated current were plotted in all the cases. The results of the data processing are given in Fig. 5.

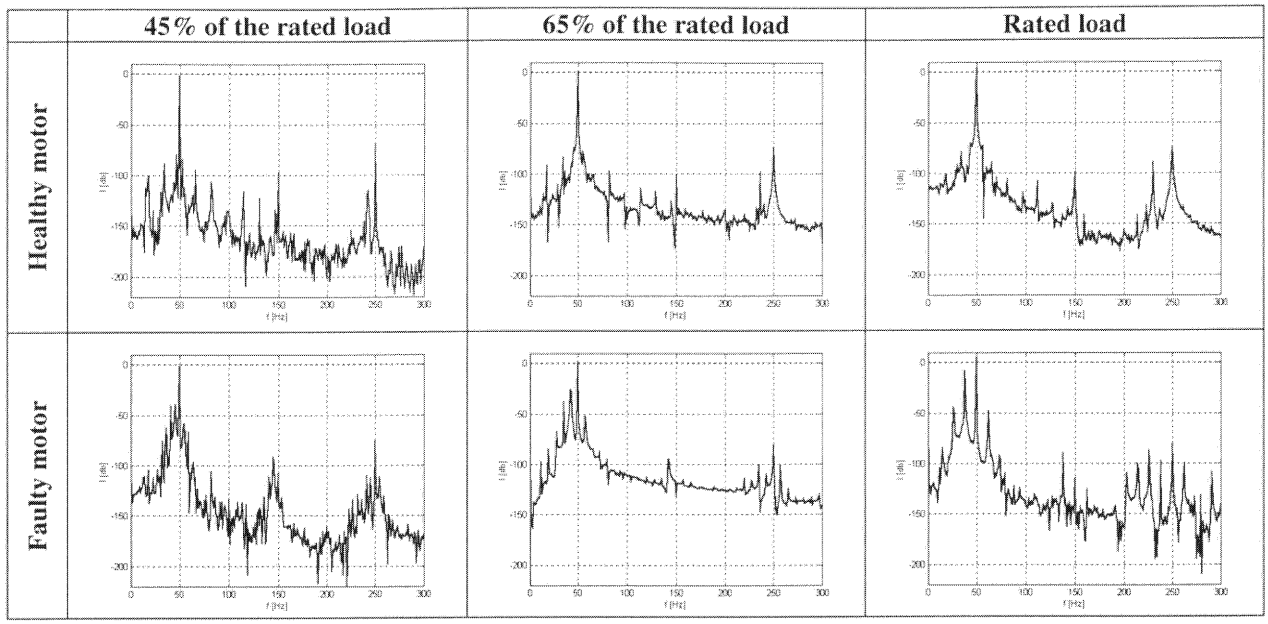

Fig. 5. The power spectrum of the measured line currents.

5. CONCLUSIONS

As it can be seen from Fig. 5. several sideband harmonics appeared in the plotted power spectrum of the line current due to the rotor fault. The frequencies of these harmonics depend on the slip and implicit of the load and can be precisely determined using equation (1).

To exemplify this the sideband harmonics in the case of the faulty motor at the rated load are highlighted in Fig. 6.

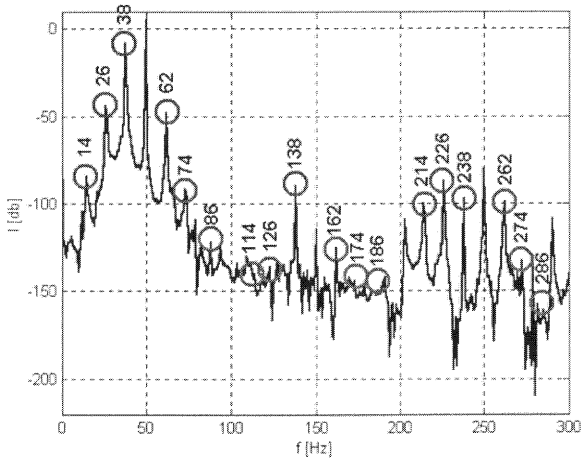

Fig. 6. The sideband frequencies of the faulty motor.

As it can be seen, almost all of the frequencies given in Table 1 were found in the analysed power spectrum. This means that both the applied diagnosis method (MCSA) and equation (1) are well suited for the proposed rotor faults detection.

The applied VIs are useful and can be utilised also to the fault detection of other type of motors.

Acknowledgement

The researches were supported by the National Council of Scientific Research in Higher Education (Romanian Ministry of Education and Research), respectively by the Sapientia Foundation (Cluj, Romania) to the authors.

REFERENCES

1. Kim, K., and Parlos, A.G., "Model-Based Fault Diagnosis of Induction Motors Using Non-Stationary Signal Segmentation," *Mechanical Systems and Signal Processing*, Vol. 16 (2002), No. 2-3, pp. 223-253.
2. Thomson, W.T., and Gilmore, R.J., "Motor Current Signature Analysis to Detect Faults in Induction Motor Drives – Fundamentals, Data Interpretation, and Industrial Case Histories," *Proceedings of 32nd Turbomachinery Symposium*, Texas A&M University, USA, 2003.
3. Milimonfared, J. et al., "A Novel Approach for Broken Rotor Bar Detection in Cage Induction Motors," *IEEE Transactions on Industry Applications*, Vol. 35 (1999), No. 5, pp. 1000-1006.
4. Szabó, L., Bíró, K.Á., and Dobai, J.B., "On the Rotor Bar Faults Detection in Induction Machines," *Proceedings of the International Scientific Conference MicroCAD '2003*, Miskolc (Hungary), Section J (Electronics and Electrotechnics), 2003, pp. 81-86.
5. Ertoglu, N., "New Era in Engineering Experiments: an Integrated and Interactive Teaching/Learning Approach, and Real-Time Visualisations," *International Journal of Education*, Vol. 14 (1998), No. 5., pp. 344-355.